UPDATE ON SRF CAVITY DESIGN, PRODUCTION AND TESTING FOR bERLinPro*

A. Neumann†, W. Anders, A. Burrill‡, A. Frahm, H.-W. Glock, J. Knobloch, O. Kugeler
Helmholtz-Zentrum Berlin, 12489 Berlin, Germany
G. Ciovati, W. Clemens, C. Dreyfuss, D. Forehand, T. Harris, P. Kneisel, R. Overton, L. Turlington
JLab, Newport News, Virginia, USA
K. Brackebusch, T. Galek, J. Heller, U. van Rienen
Rostock University, 18059 Rostock, Germany
E. Zaplatin
Forschungszentrum Jülich, 52425 Jülich, Germany

Abstract

The bERLinPro Energy Recovery Linac (ERL) is currently being built at Helmholtz-Zentrum Berlin in order to study the accelerator physics of operating a high current, 100 mA, 50 MeV low emittance ERL utilizing all SRF cavity technology. For this machine three different types of SRF cavities are being developed. For the injector section, consisting of an SRF photoinjector and a three two cell booster cavity module, fabrication is completed. The cavities were designed at HZB and manufactured, processed and vertically tested at Jefferson Laboratory. In this paper we will review the design and production process of the two structures and show the latest acceptance tests at HZB prior to installation into the newly designed cryo-module. For the Linac cavity the latest cavity and module design studies are being shown.

CAVITY TYPES FOR bERLinPro

Helmholtz-Zentrum Berlin is currently designing and building a high average current all superconducting CW driven energy recovery linac (ERL) as a prototype to demonstrate low normalized beam emittance of 1 mm·mrad at 100 mA and short pulses of about 2 ps [1]. The injector section (see Figure 1) consists of a 1.4-cell photo-injector cavity [2] using a high quantum efficiency normal conducting multi-alkali cathode and three high power 2-cell booster cavities of Cornell type [3]. The photo-injector will deliver 2.3 MeV kinetic energy, two booster cavities 2.1 MeV each whereas the third is operated in zero crossing to impose an energy chirp for bunch compression. This beam is fed via the merger section into the recirculator consisting of a string of three linac cavities, where the beam is accelerated to 50 MeV and in a second pass its energy is recuperated. According to their role in this machine the requirements and such the SRF properties of these three cavity types vary:

- **The Gun** cavity needs to deliver high on axis fields close to the cathode within the half-cell to suppress beam emittance dilution by space charge. Further an effective RF power to beam energy conversion at a field level as high as possible is required, as the cavity will experience the full beam-loading of 100 mA and the foreseen transmitters power and coupler power handling will be limited to 230 kW [4]. To achieve this, a high beam emission phase between laser pulse and RF field is mandatory and was achieved by having a $0.4\times\lambda/2$ half cell. This was optimized for low peak fields to avoid field emission, especially from the cathode area, as here emitted electrons have the highest probability to leave the structure.

- **The Booster** cavity design relies on the proven concept of Cornell's 2-cell injector cavity. The design was altered in order to house a pair of modified KEK c-ERL couplers since higher power than in the Cornell case and stronger coupling than in the KEK case were needed. This was achieved by introducing a golf tee shaped antenna tip which also helps in mitigating coupler kicks and related emittance deterioration [5] and by also increasing the one beam tube diameter to 88 mm.

- **The Linac** cavity needs to operate at high CW fields of E_{acc} of 20 MV/m, at best experiences no net beam-loading and can thus be operated at a narrow bandwidth, but experiences still the Wakes of two high current with respect to the $TM_{010\text{-}\pi}$ mode by π shifted beams. Thus this design needs to be a very good compromise with respect to both, low peak field ratios, a high impedance for the fundamental mode and maximum higher order mode (HOM) propagation and damping. Often these design features have opposite requirements with respect to the geometry. The cavity is thus a combination [6] of Cornell's mid-cell shape and the waveguide based HOM damping approach of JLab. Here, one port is sacrificed to install a variable coaxial coupler of TTF-III type.

Table 1 summarizes all RF design properties of the three structures and first measured properties in vertical (VTA) or horizontal (HTS) set up already after welding the helium vessel (HV) for the gun and booster cavities. The two latter were both fabricated and processed at JLab and delivered

* Work supported by German Bundesministerium für Bildung und Forschung, Land Berlin, and grants of Helmholtz Association
† Axel.Neumann@helmholtz-berlin.de
‡ Now at SLAC

with HV to HZB where first tests with the same critically coupled antenna should confirm the level of performance achieved with the last vertical tests at JLab. All quality factor (Q_0) measurements presented here were done at 1.8 K.

The gun is one of the most critical components and in order to mitigate risk, it is being developed in several stages. The prototype presented here is a medium power version of the final high power structure and thus utilizes CW modified TTF-III couplers. The values in brackets are given for this cavity called Gun1.0. Figure 2 displays an overview of the current status of all three cavities. The gun cavity has been already tested several times with the JLab antenna configuration, the first booster cavity awaits the first horizontal test while three more are on their way to Germany and the linac cavity RF design is accomplished. In this paper

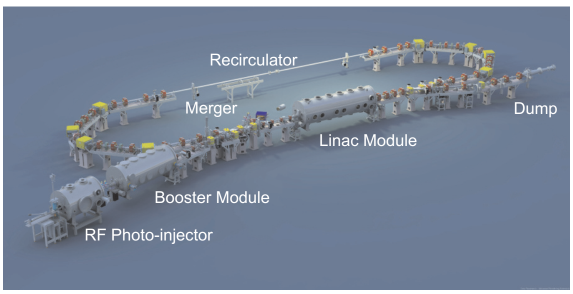

Figure 1: The bERLinPro Energy Recovery Linac machine layout with the three cavity types cryo-module displayed in greyish color.

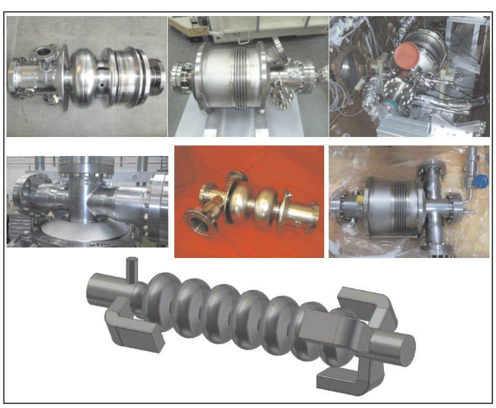

Figure 2: This set of pictures displays an overview and current status of the bERLinPro SRF cavities. The gun (upper row) performed its first horizontal test, the 1st booster cavity (mid row) arrived at HZB and the Linac's design phase is being finalized.

the latest developments since spring this year are reported. For previous production and processing history please refer to [7–9].

[1] For the Gun cavity field ratios E_{acc} needs to be replaced by E_0.

GUN CAVITY HORIZONTAL TESTS

After the cavity fabrication the prototype experienced a long history of testing and processing in order to achieve the requirements by bERLinPro. As this cavity was a new design utilizing the rather complex cathode insert and non-resonant bandstop-filter like choke cell structure of HZDR [10] the production was challenging and the prototype did not fully meet the design geometry as was shown by CMM measurements. From those data a new RF model was made and it was concluded that R/Q and the geometric constant G was reduced by about 11-12% whereas the field ratio E_{peak}/E_0 increased by 15% (E_0 is the peak on axis longitudinal electric field). Further an increase of multipacting probability and lowering of the onset field was observed by CST PS PIC [11] simulations, which was confirmed by the last vertical tests as well as OST based quench measurements. Like the simulation, the latter showed that activity and thus quench happen in the half cell's equator dome, whereas multipacting is probably triggered by field emission originating closer to the inner iris and pointing inwards into the half cell. After welding of the helium vessel, the cavity reached a performance close to the design specifications. So it was decided to ship the cavity to HZB.

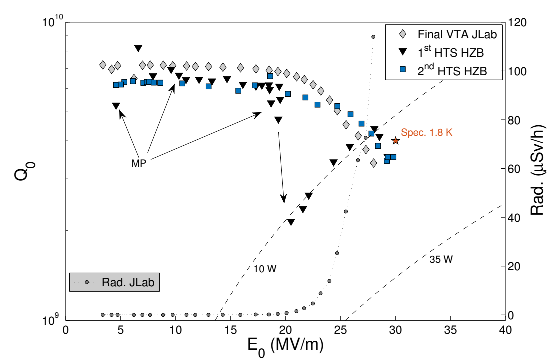

Figure 3: Quality factor versus on axis peak field at 1.8K for the prototype gun cavity of the last VTA test at JLab (grey diamonds) and first horizontal tests at HZB (black triangles, blue squares). The radiation level recorded during the VTA test is shown by grey circles.

Figure 3 shows a comparison of the $Q_0(E_0)$ data taken during the latest VTA test at JLab including measured radiation pointing at a field emission onset at 16-18 MV/m. The first power rise at HZB having the cavity with the same antennas mounted horizontally in HoBiCaT [12] as received shows a lot of multipacting activity, especially at 18 MV/m where the peak response was also expected by simulation. After RF processing, by coincidence along the 10 W line, the JLab data could be finally confirmed in a second test with a clean power rise shown by the blue squares. The helium vessel still needed some modifications to its surface, so a test was scheduled in order to confirm the cavity performance. Unfortunately the cavity was for a short time exposed to a connecting hose of the vacuum system which was in an undefined state at that time. Therefore, an additional

ISBN 978-3-95450-178-6

Table 1: Cavity type, calculated parameters and properties measured with helium vessel for bERLinPro. *Italic case* values in brackets shows deviations of the Gun1.0 prototype from the design, non-italic in brackets are design parameters of the medium power prototype gun.

Design Parameter	**Gun**	**Booster**	**Linac**
Type of operation	CW, high beam power, high peak on-axis field	CW, high beam power, intermediate acc. field	CW, high beam current high acc. field
Number of cells	$1.4\times\lambda/2$	$2\times\lambda/2$	$7\times\lambda/2$
$TM_{010\text{-}\pi}$ frequency (MHz)	1300	1300	1300
Operating temperature (K)	1.8	1.8	1.8
Beam current (mA)	100 (4)	100	$2\times$ 100
HOM absorber	beam tube	beam tube	waveguide + beam tube
FPC type	twin modified c-ERL (TTF-III)	twin modified c-ERL	single modified TTF-III
Energy gain/cavity (MeV)	2.3 (3.5)	2.1	14.8
Beam emission or RF phase (deg)	40-60	-90 and 0	-15
$R/Q_{\parallel}$ for $\beta = 1$ (Ω)	150 (*132.5*)	219	788
Geometry factor G (Ω)	174 (*154*)	261	266
E_{peak}/E_{acc} [1]	1.45 (*1.66*)	2.02	2.08
B_{peak}/E_{acc} [1] (mT/MVm^{-1})	3.2	4.44	4.40
Q_{loaded} for $TM_{010\text{-}\pi}$	$1.1\cdot10^5$ ($3.6\cdot10^6$)	$1.05\cdot10^5$	$5\cdot10^7$
Max. Q_{ext} 1st TM dipole band	$11\cdot10^3$	170, 7300	$\leq 8\cdot10^3$
$P_{forward}$ at $\Delta f = 0$ (kW)	230 (up to 5.8)	230	1.4
$\Delta f/\Delta P$ (Hz/mbar)	20	5	not calculated yet
Measured Properties with HV	**Gun**	**Booster**	**Linac**
Peak on axis electric field (MV/m)	34.5	34-40	NA
Peak surface electric field (MV/m)	57.3	34.4-40.4	NA
Peak magnetic field (mT)	110.4	75.5-89	NA

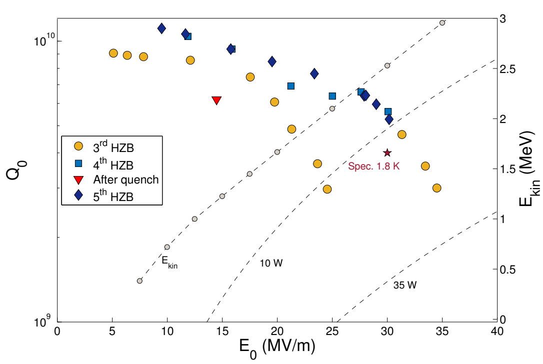

Figure 4: Quality factor versus on axis peak field for the prototype gun cavity of the latest horizontal tests at HZB. The grey circles with dashed line shows the kinetic energy gained at the corresponding field level. All tests were at 1.8K

test was also needed to check whether the cavity surface got contaminated. Figure 4 depicts a summary of the latest tests after that incident. In first attempts it was impossible to obtain fields above some low level and even pulsing the cavity to obtain the coupling β_c failed and the cavity showed a multipacting-like behavior with a following quench afterwards. In a second attempt (yellow circles) it was possible to stabilize the cavity by RF processing. Especially between 24 and 30 MV/m where with constant forward power the transmitted power increased while the observed radiation decreased some emitters were removed by processing. Here, the cavity reached its maximum field of 57.3 MV/m on the surface which led to a quench. By thermal cycling above T_C the Q_0 could be recovered, as the quench led to trapped magnetic flux of the RF field. A following test showed a slightly improved surface resistance, but the cavity now quenches right above the design field level. Nevertheless, as this cavity will reach the beam energy to be studied within the bERLinPro gun program, it will be installed in the first gun module for first beam tests in the Fall of next year.

FINAL BOOSTER CAVITY VERTICAL TESTS

As an update from Ref. [9] two more cavities received their HVs after the vertical tests showed very good results beyond the required level needed for bERLinPro, as can be seen in Figure 5. Good performance was achieved even though two cavities had a hole in the equator weld after electron beam welding which had to be repaired. Figure 6 summarizes the test after HV welding for the three cavities which will be installed to the cryo-module. They all outperform the specs and field emission onset is above the design

ISBN 978-3-95450-178-6

Table 2: Mechanical properties of gun and booster cavity simulated [13] and measured for the different set ups during testing (HV: Helium vessel).

Cavity and set up	$\Delta f/\Delta P$ (Hz/mbar)	$\Delta f/(E_{\mathrm{acc}})^2$ (Hz/(MV/m)^2)
	Booster	
VTA	-205	-7.1
VTA + HV	-278	-6.5
Simulated VTA + HV	-180	NA
Simulated HV+tuner	≈5	-2.2 [3]
	Gun	
VTA	-601	-5.2
VTA + HV	-561	-4.7
Simulated VTA +HV	-550	NA
HV+threaded rods	150	-3.7
Simulated HV+tuner	≈5-10	NA

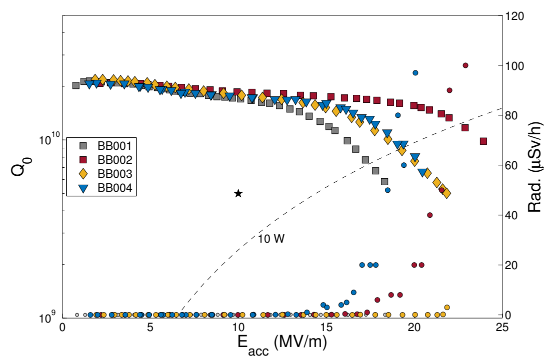

Figure 5: Quality factor (Q_0 versus mean accelerating field E_{acc} at 1.8K for the four booster cavities produced for bERLinPro in vertical set up at JLab before HV welding. All cavities outperform the specifications. As a reference the 10 W loss level is shown. The circles denote the corresponding radiation measured.

field level of E_{acc} of 10 MV/m. An open issue which needs to be checked are helium leaks which opened below the lambda point at two cavities and most probably appeared at the NbTi flanges of the power couplers. In the module configuration those leaks would only see vacuum on both sides. Table 2 gives an overview of the measured helium pressure and Lorentz force detuning sensitivities of the gun and booster cavities. The values measured so far were mostly confirmed by ANSYS simulations given in the same table which gives confidence that the low $\Delta f/\Delta P$ ratios aimed for are within reach. Especially the zero crossing seen for the gun cavity between the VTA and HTS set up demonstrates the possible close-to-zero value for correct tuner-HV boundary conditions.

THE LINAC CAVITY STATUS

The Linac cavity's RF design was finalized last year, but the HOM and FPC port configuration showed to impose an unacceptable high increase in emittance to the 6.5 MeV beam from the injector. This was solved by tapering the rectangular waveguide penetrating the beam tube. By that the increase was reduced from about 10% to lower than 1% which is not shown here. Further, the geometry variation due to production tolerances and following different cell tuning to achieve field flatness and target frequency was studied to estimate the impact of HOM's frequency spread on beam break-up by transverse dipole-like modes. A perturbation based method [14] was applied to calculate the frequency and shunt impedance spectrum of eight different end-cell geometry candidates which all have similar field flatness and target frequency [15]. The result is partly shown in Figure 7 which displays the frequency spread of all eight candidates. Note, that this calculation was done without the waveguide ports, as this would take too much computational effort. Still a variation for each type of mode can be extracted as the type was identified by an automatized mode recognition algorithm [16]. The dipole mode frequency spread is about 1.3 MHz rms, for all the three type of modes

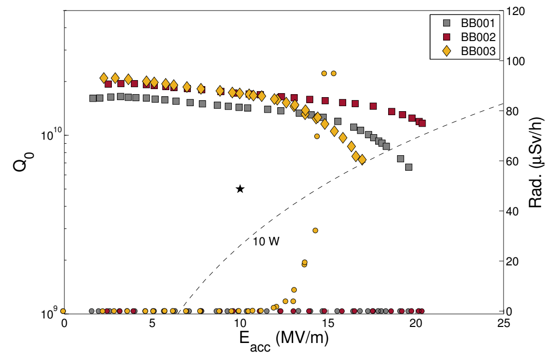

Figure 6: Q_0 versus E_{acc} measurement of cavity 1-3 as in Figure 5 now after helium vessel welding. The circles denote the corresponding radiation measured. All data was taken at 1.8K, except for BB001 at 2.0K.

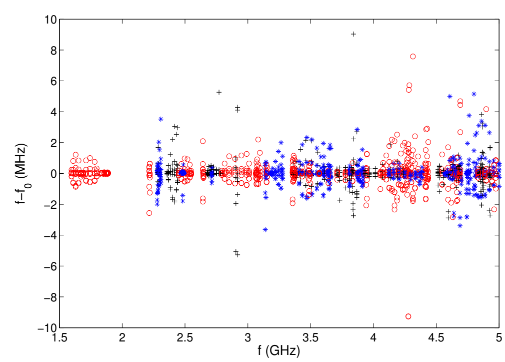

Figure 7: Frequency variation of higher order modes by geometry variations of the end-cell for field-flat tuned bERLinPro linac cavities calculated by a perturbation method described in [14]. Black crosses: Monopoles, red dots: Dipoles, blue stars: Quadrupoles.

shown here it is about 1.35 MHz rms. This number will be used for further beam break-up studies once the impedance spectrum of the module as a coupled system is known. In total the spectrum up to 7.1 GHz was calculated including the azimuthal variation up to decapole order.

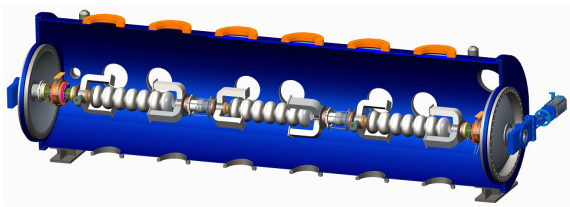

Figure 8: Possible layout of the three cavity Linac module including beam tube absorbers at both ends.

As the impedance budget and transverse dipole-like modes mainly determine the threshold current until beam break-up occurs [17], the cavity module needs to be studied as a coupled system. A possible layout of the module is shown in Figure 8. It consists mainly of the three 7-cell cavities with the coaxial FPC and waveguides for HOM damping and beam tube absorbers at the module exits to collect all HOM power traveling downstream via the enlarged beam tubes. The orientation will be chosen to minimize coupler kicks [6] and to cover all polarization of HOMs by proper neighboring of the waveguide orientation between two cavities. First studies using CST'S Wake Field solver [11] were performed in order to rule out unwanted modes in the connecting beam tube between two cavities. The result is displayed with the simulation settings in Figure 9 for different beam tube distances. Except the TM_{020} band there are no modes close to beam harmonics. Any resonant high impedance interaction at the aforementioned monopole passband was ruled out by intense eigenmode simulations within that frequency range.

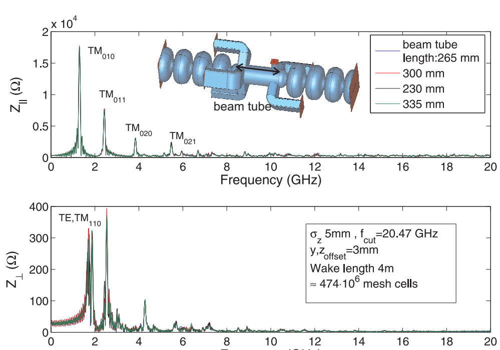

Figure 9: Wake study to search for trapped modes within the interconnecting beam tube section between two cavity structures for different lengths. The upper plot depicts the longitudinal impedance, the lower the transverse respectively. Beam harmonics would appear at a multiple of 1.3 GHz.

OUTLOOK

The next steps will be the assembly of the cold mass of the first gun cavity and first horizontal tests under module like conditions in the HoBiCaT test stand. Also the first booster cavity is prepared for its first horizontal test still with critical coupling to confirm the latest JLab results. The Linac structure will be studied with respect to concatenation [18] at Rostock University until the end of this year to optimize the module layout. In parallel the integration of the cavity and waveguide end-groups within the helium vessel is ongoing.

REFERENCES

[1] M. Abo-Bakr et al., IPAC'15, Richmond 2015, TUPWA018, p. 1438 ff., Virginia, USA (2015)

[2] A. Neumann et al., IPAC'13, Shanghai 2013, MOPFI003, p. 285 ff. , China (2013).

[3] M. Liepe, Proc. of SRF'09, MOOBAU04, p. 27 ff., Berlin, Germany (2009).

[4] V.F. Khan et al., LINAC'14, Geneva, 2014, TUPP065, p. 575ff, Switzerland (2014).

[5] A. Neumann et al., IPAC'14, Dresden 2014, WEPRI007, p. 2490 ff., Germany (2014).

[6] A. Neumann et al., LINAC'14, Geneva, 2014, MOPP070, p. 217ff, Switzerland (2014).

[7] A. Burrill et al., IPAC'14, Dresden 2014, WEPRI005, p. 2484 ff., Germany (2014).

[8] A. Burrill et al., IPAC'15, Richmond 2015, WEPMA011, p. 2768 ff., Virginia, USA (2015).

[9] A. Burrill et al., IPAC'15, Richmond 2015, WEPMA010, p. 2765 ff., Virginia, USA (2015).

[10] A. Arnold et al., Nucl. Instr.and Meth. A 577 (2007) 440-454

[11] CST AG, Particle Studio®, Darmstadt, Germany.

[12] O. Kugeler et al., REVIEW OF SCIENTIFIC INSTRUMENTS 81, 074701 (2010).

[13] E.N. Zaplatin et al., IPAC'13, Shanghai 2013, WEPWO009, p. 2328 ff. , China (2013).

[14] K. Brackebusch, U. v. Rienen, Proceedings of Compumag 2015, Montréal, Québec, Canada (2015)

[15] T. Galek et al., IPAC'13, Shanghai, 2013, WEPWO010, p. 2331ff, China (2013).

[16] K. Brackebusch et al., Proc. of IPAC'14, MOPME014, p. 409 ff., Dresden, Germany (2014).

[17] G.H. Hoffstaetter, I.V. Bazarov, and Ch. Song., Phys. Rev. ST Accel. Beams, 10:044401, Apr 2007.

[18] T. Flisgen, H.-W. Glock, U. van Rienen: Compact Time-Domain Models of Complex RF Structures Based on the Real Eigenmodes of Segments. IEEE Transactions on Microwave Theory and Techniques, Vol. 61, No. 6, pp. 2282-2294, June 2013. DOI: 10.1109/TMTT.2013.2260765.

ISBN 978-3-95450-178-6